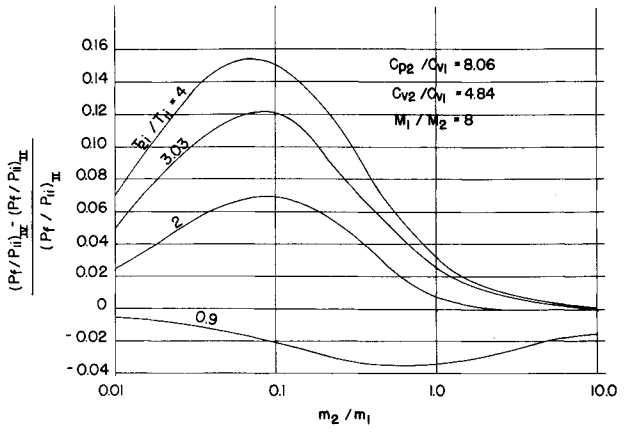

Fig. 3 Comparison of results for cases 2 and 4.

mass ratio. To show this analytically, write Eq. (14) as

$$\left(\frac{C_{v2}}{C_{v1}}\right)\left(\frac{M_2}{M_1}\right)\left(\frac{P_f}{P_{1i}}\right) - \left(\frac{C_{p2}}{C_{v1}}\right)\left(\frac{T_{2i}}{T_{1i}}\right)\left(\frac{m_2}{m_1}\right) - 1 = \left[\left(\frac{C_{v2}}{C_{v1}}\right)\left(\frac{M_2}{M_1}\right) - 1\right]\left(\frac{P_f}{P_{1i}}\right)^{\frac{K-1}{K}} \quad (15)$$

Now for large values of (m_2/m_1), the unity term on the left-hand side and the entire right-hand side of the equation are negligible. Solving for the pressure ratio from the remaining equation yields

$$P_f/P_{1i} = (C_{p2}/C_{v2})(T_{2i}/T_{1i})(M_1/M_2)(m_2/m_1)$$

Not only is this a linear relation, but it is the identical relation found for case 2.

If the barrier in case 4 were removed, the end state would be the same as that of case 2, assuming that the initial conditions were the same in both cases. Thus, the change in pressure in going from the end state of case 4 to the end state of case 2 can be associated with the mixing. In this manner the change in pressure due to charging and that accompanying mixing can be separated and the latter evaluated. A plot of the change in pressure accompanying mixing is given in dimensionless form in Fig. 3. Interest in results such as these provided the initial stimulus for this investigation.

It is of interest to examine the four special situations discussed in the section on case 1. These are a) two gases are the same and $T_{2i}/T_{1i} = 1$; b) two gases are the same and $T_{2i}/T_{1i} \neq 1$; c) two gases are different and $T_{2i}/T_{1i} = 1$; and d) two gases are different and $T_{2i}/T_{1i} \neq 1$.

It was found in case 1 that only (d) yielded a change in pressure upon mixing. Now examine these four situations with regard to the pressure change associated with mixing in the charging arrangement, i.e., that in going from the end state of case 4 to the end state of case 2.

For situation (a), Eq. (13) yields $P_f/P_{1i} = 1 + (C_p/C_v)(m_2/m_1)$, whereas Eq. (15) yields the same result. Thus, the change in pressure accompanying the removal of the barrier thereby going from the final state of case 4 to the final stage of case 2 would be zero.

Now examine situation (b). Equation (13) becomes

$$P_f/P_{1i} = 1 + (C_p/C_v)(T_{2i}/T_{1i})(m_2/m_1)$$

This result is also found by use of Eq. (15). Thus, if the two gases are the same, there will be no pressure change associated with the mixing regardless of the initial temperatures.

In general, there will be a pressure change accompanying the mixing process for situations (c) and (d).

High-g Resistant Electronic Fuse for Projectile Payloads

WILLIAM H. MERMAGEN*
Ballistic Research Laboratories, Aberdeen Proving Ground, Md.

GUN-LAUNCHED projectiles have placed payloads at high altitudes[1] for sounding, seeding, and performance experiments,[2,3] creating a need for a 60,000 g time-delay fuse with delays as long as several minutes. Electronic delay circuits with high-g components became available during the last decade, can be temperature compensated, assembled with ease, calibrated, pretested, and manufactured at costs comparable to pyrotechnic devices. This Note describes the development of such fuses.

Fuse Design

Electrical

In 1967 a very sensitive, programable, unijunction transistor (PUT)[4] became commercially available. This transistor, the D13T2, has excellent voltage sensitivity, low leakage, capability for operation down to 2 v d.c., is inexpensive and comes in a solid plastic T0-98 case.

The timing circuit (Fig. 1) was designed around the D13T2, a PNPN device which operates as a triode thyristor. It has a gate-controlled diode section which becomes highly conductive at the appropriate anode-gate voltage. Once the diode section begins to conduct, the regenerative characteristics of the PNPN junction cause the D13T2 to switch on. At the same time a high energy pulse appears at the cathode and can be used to trigger other devices such as a silicon-controlled rectifier (SCR).

The circuit in Fig. 1 can provide time delays up to several minutes by changing the R_1C_1 time constant. The D13T2 turns on when the anode potential is 0.41 v higher than the gate. The gate potential is determined by the battery and the ratio of resistances in the divider network. The anode potential is directly the potential across capacitor C_1. After power is applied, the capacitor C_1 begins to charge and the anode voltage increases until it exceeds the intrinsic standoff potential. Then current begins to flow from anode to gate. The diode section of the D13T2 begins to conduct, regeneration takes place and the PUT is switched on. A fast-rising,

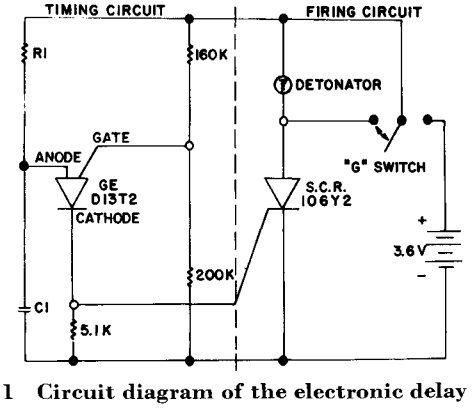

Fig. 1 Circuit diagram of the electronic delay fuse.

Received December 15, 1970; revision received April 22, 1971.
* Chief, Physical Measurement Section, Exterior Ballistics Laboratory. Member AIAA.

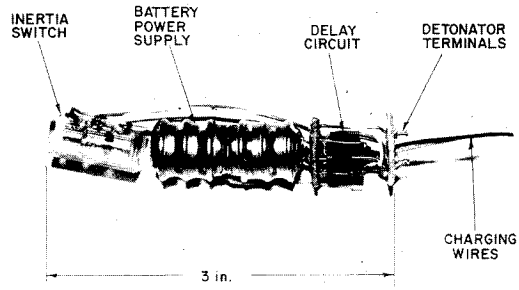

Fig. 2 The electronic delay fuse before potting.

high energy pulse appears at the cathode and is used to trigger the SCR (C106Y2). With the SCR triggered, the battery, detonator and SCR form a closed circuit, and maximum battery current can flow through the detonator.

The repeatability of the delay circuit depends on the sensitivity of the D13T2 and can be enhanced by choosing the divider network ratio (0.8) so that the anode reaches standoff while the charging potential is still a nearly linear function of time. The circuit always fires at the same potential within mv regardless of time constant indicating the good sensitivity of the transistor.

Mechanical

Different types of miniature batteries were tested including alkaline, silver-zinc, mercury, and nickel-cadmium cells. Only nickel-cadmium cells could supply the current needed and survive the gun accelerations. NiCad cells were rated at 50 mah and yet were able to supply 1.4 amp into a 2 Ω load for 2 sec, an ample amount of time to insure that the detonator would be set off. These cells have the advantage of being rechargeable and can be tested prior to assembly as well as after manufacture of the fuse. Figure 2 is a photograph of the battery pack as well as the fuse assembly.

The complete fuse had to fit into a cylindrical cavity 1.9-cm diam by 11.5 cm deep. The gun-launch was expected to produce accelerations up to 60,000 g for durations in the order of 10 msec. The fuse had to turn on at launch and be unaffected by the shock of launch. Selection of components, potting techniques, and turn-on as well as safety devices were influenced by these considerations.[5]

The Ballistic Research Laboratories (BRL) lead impact test facility[6] was used to impose a controlled acceleration profile on the active components of the fuse. Repeated tests at 60,000 g showed that the D13T2 PUT and the C106Y2 SCR devices could survive and function reliably when completely immersed in potting compound. A variery of detonators, however, failed to survive except for the NND-211.[7] The NND-211 is physically small in size, can ignite a booster charge of composition C-4 at a standoff distance of 1.5 cm, and is insensitive to static charge.

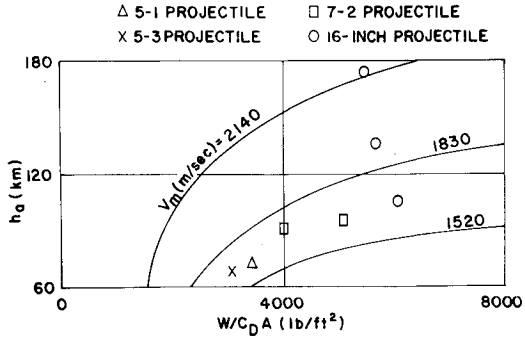

Fig. 3 Apogee as a function of ballistic coefficient with muzzle velocity as a parameter.

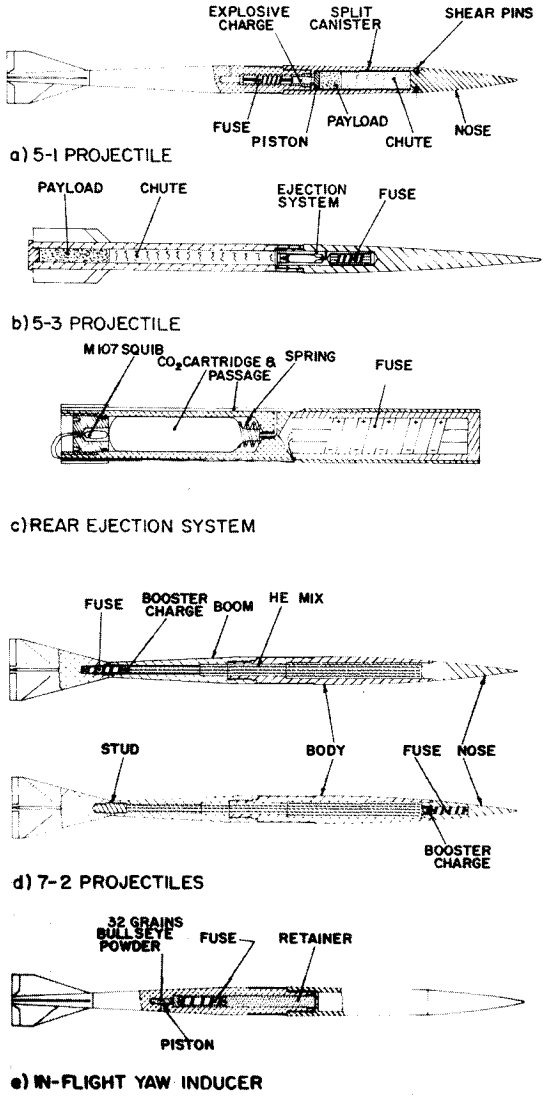

Fig. 4 Mechanical configurations of various projectiles and fuse systems: a) mechanical assembly of parachute-payload ejection system (5-1 projectile); b) the 5-3 probe projectile with rear ejection system; c) details of the rear ejection system; d) the 7-2 projectile filled with HE mix with two different fuse locations; and e) in-flight yaw inducer.

The components of the fuse must be potted to enable them to survive high accelerations. It is necessary to assure that the potting material has flowed around all the components, since any voids could allow components to move and break during launch. An exposy resin (Epon 815) with a liquid polymer (Thiokol LP-3) added to reduce brittleness was used in a 3:2 EPON/LP ratio by weight as a potting agent. The potting material must cure for several days.

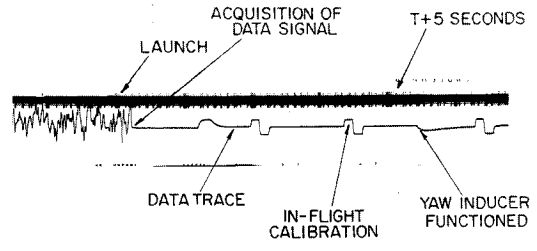

Fig. 5 Sample data trace from a dynamic stability flight of a 5-1 probe with yaw inducer.

Applications

The electronic delay fuse has been used to eject payloads from projectiles, to disturb projectiles in flight, and to detonate high explosives in the upper atmosphere. Since the fuse is used in a high-g environment, the projectile configurations are important.

Test vehicles

Figure 3 shows the ballistic performance of a variety of HARP[2] projectiles. The curves indicate the expected apogee versus ballistic coefficient, W/C_DA, with muzzle velocity as parameter. The plotted points indicate achieved apogees. The 7-2 projectile can achieve 100 km and perform seeding experiments in the sporadic-E layer of the ionosphere.

In the 5-1 vehicle the fuse is in midsection (Fig. 4a) and detonates a charge of black powder when the shell is near apogee. During launch, the nose has been held on to the projectile by a set of shear pins. At initiation, the gas pressure behind the piston drives a split canister containing the payload forward. The canister transmits the force to the base of the nose. The retaining pins are sheared and the canister is ejected. The split halves separate allowing the parachute to deploy.

The timing accuracy needed depends on the time the projectile spends near apogee. For a nominal pogee of 70 km and a launch elevation of 80° a 2-sec error in fuse time will cause a 30-m error in ejection altitude; 10 sec, 500 m. Comparable timing errors near launch result in distance errors in the order of tens of kilometers, since the velocity is greatest at the extremes of the trajectory.

The electronic delay fuse was used on 45 flights of the 5-1 projectile, and on only 3 flights did the set times differ from the actual function times by as much as 2 sec (on 120–140 sec). One flight had a complete failure to function. The fuse performance times were obtained from radar observations of the ejection event.

The 5-3 projectile is a modified 5-1 vehicle designed to eliminate the debris resulting from ejection so that the 5-3 can be used for upper atmosphere experiments near populated areas. The 5-3 ejects its payload out the rear (Fig. 4b) with only a lightweight cylindrical plug as debris. Parachute and payload are ejected by gas from a CO_2 cartridge which is burst at apogee. The safety of the fuse is increased since, instead of a detonator, it uses an electromechanical arrangement (Fig. 4c). The output terminals of the fuse are connected to a low-energy, M107 squib. When the fuse functions near apogee, the squib is set off and the force of the gases drives the CO_2 cartridge against the holdoff spring into a pin. The pin ruptures the seal on the CO_2 cartridge and the holdoff spring returns the cartridge to its original position. The gas content of the cartridge is free to flow through the CO_2 passage to expel the parachute and payload.

Seeding of the upper atmosphere

The 7-2 projectile,[8] launched from a smoothbore, 175 mm gun, is the vehicle for carrying a high explosive payload to apogees of from 95 to 105 km. The high-altitude performance of this shell is based on a muzzle velocity of 1580 m/sec. The empty shell weighs 14 kg and carries an explosive payload of 2 kg. For seeding experiments the payload has been a mixture of RDX, TNT, and cesium nitrate. Detonation at apogee creates a cloud of electrons and ions which are transported by upper atmosphere winds and the Earth's magnetic field.

At first, the fuse was located in the stud of the projectile ahead of the fins to maximize payload volume. Difficulties with this arrangement forced a redesign with the fuse and booster located in the nose (Fig. 4d). With the fuse located in the rear, it would either function at the wrong time or not at all. The sporadic performance varied from −58 to +72 sec (140-sec fuse). To eliminate the possibility of aerodynamic heating particularly at the fin surfaces, the projectile was coated with an ablating compound designed to keep the surface at less than 110°C. Tests of the change of fuse timing due to thermal effects were made. The firing time stayed within ±5% of the preset time at temperatures up to 120°C. At higher temperatures degradation in fuse performance and erratic behavior were observed. Unfortunately, subsequent test flights of the 7-2 vehicle with ablative coatings did not show an improvement. The sporadic results are perplexing since the fuse behaves properly in the midsection of a 5-1 or 7-2 vehicle.

Yaw inducer

A program to determine the flight stability and the aerodynamic coefficients of projectiles under real trajectory conditions has been underway for several years at the BRL.[9] The flight of a projectile is perturbed at a known altitude and its subsequent dynamical behavior is observed using solar aspect sensors or accelerometers with on-board telemetry. The electronic delay fuse has provided a timing pulse to drive the yaw inducer which produces the in-flight disturbance.

The projectile is induced to yaw by ejecting a brass slug out the side so that a side moment results. The arrangement of slug, powder charge, and fuse is shown in Fig. 4e. The slug is press fit into a hole located as far from the center of mass of the projectile as possible for maximum overturning moment. The hole is drilled to leave a thin diaphragm in the shell wall. The powder gases are restrained until a sufficiently high pressure ruptures the diaphragm giving a "shot start" to the slug.

Such a short barrel arrangement has produced slug velocities as high as 305 m/sec, almost the speed of sound in air. When used with the 5-1 projectile at an altitude of 6 km and a projectile velocity of 1500 m/sec, a yaw of from 3° to 4° results. At higher altitudes or lower projectile velocities greater yaw angles are produced. With initial projectile velocities in the order of 1500 m/sec, each second of error in fuse timing means that the vehicle has traveled more than a kilometer along its flight path. The electronic delay fuse has successfully initiated the yaw inducer with 0.5 sec accuracy at delays from 5 to 10 sec. The 5-1 projectile has been induced to yaw in flight on five separate tests with data on aerodynamic performance resulting. The fuse functioning times were determined by both radar observations and telemetered yaw data.

Figure 5 shows a data channel from an accelerometer-instrumented flight and timing pulses from a range timing oscillator. After launch the data signal is acquired. In-flight calibrations insure that the accelerometer calibration is known after launch. The fuse had been set for a delay of 5.0 sec. At T + 5.5 sec the accelerometer shows that the projectile was disturbed and hence that the yaw inducer functioned.

References

[1] Murphy, C. H. and Bull, G. V., "Gun-Launched Probes Over Barbados," *Bulletin of the American Meteorological Society*, Vol. 49, No. 6, June 1968, pp. 640–644.

[2] Boyer, E. D., "Five-Inch Gun Meteorological Sounding Site, Highwater, Quebec," MR-1929, AD 673 712, July 1968, Ballistic Research Labs., Aberdeen Proving Ground, Md.

[3] Mermagen, W. H., Cruickshank, W. J., and Vrataric, F., "VHF and UHF High-G Telemetry for HARP Vehicles," *The Fluid Dynamics Aspects of Ballistics Conference Proceedings No. 10*, Advisory Group for Aerospace Research & Development, 1966.

[4] Spofford, W. R., Jr., "The D13T2—A Programmable Unijunction Transistor," Application Note 90.70, Nov. 1967, General Electric, Syracuse, N.Y.

[5] Evans, J. W., "Development of Gun Probe Payloads and a 1750 Mc/s Telemetry System," MR-1749, AD 637 747, May 1966, Ballistic Research Labs., Aberdeen Proving Ground, Md.
[6] Marks, S. T., Pilcher, J. O., and Brandon, F. J., "The Development of a High Acceleration Testing Technique for the Electronic Instrumentation of HARP Projectile Systems," MR-1738, AD 635 782, March 1966, Ballistic Research Labs, Aberdeen Proving Ground, Md.
[7] Caudill, G. H., Taylor, B. C., and Melani, G., "The Development of an Improved Electric Detonator," MR-1684, AD 477 112, August 1965, Ballistic Research Labs., Aberdeen Proving Ground, Md.
[8] Boyer, E. D. and MacAllister, L. C., "Seven-Inch HARP Gun-Launched Vertical Probe System: Initial Development," MR-1770, AD 640 825, July 1966, Ballistic Research Labs., Aberdeen Proving Ground, Md.
[9] Mermagen, W. H., "Measurements of the Dynamical Behavior of Projectiles Over Long Flight Paths," AIAA Paper 70-538, Tullahoma, Tenn., May 1970.

Attitude Motion in an Eccentric Orbit

D. K. Anand,* R. S. Yuhasz,† J. M. Whisnant‡
Johns Hopkins University, Applied Physics Laboratory, Silver Spring, Md.

I. Introduction

In a previous paper[1] the capture and stability of a gravity-gradient satellite in an eccentric orbit was reported. A stroboscopic[2] study of the motion at apogee was conducted and it was shown that the satellite could be captured by magnetically steering the satellite into the stable region. This note reports the results of further stroboscopic as well as analytical studies of the oscillations and stability regions of a gravity-gradient satellite in an eccentric orbit.

II. Analysis

Satellite oscillations in the plane of an elliptic orbit are described by[3,4]

$$(1 + e\cos\nu)(d^2\varphi/d\nu^2) - 2e\sin\nu(d\varphi/d\nu) + \omega^2\sin\varphi\cos\varphi = 2e\sin\nu \quad (1)$$

where e is the orbital eccentricity, $\omega^2 = 3[(I_x - I_z)/I_y]$, φ is the pitch libration angle measured from the local vertical, ν is the true anomaly and I_x, I_y, I_z are the principle moments of inertia. This equation has been investigated by researchers using both numerical integration and phase space representations. Here we consider a perturbational technique.

The term $\sin\varphi\cos\varphi$ in Eq. 1 may be expanded in a Maclaurin series so that the pitch equation becomes

$$(d^2\varphi/d\nu^2) + \omega^2\varphi = 2e\sin\nu + 2(d\varphi/d\nu)e\sin\nu - (d^2\varphi/d\nu^2)e\cos\nu + \tfrac{2}{3}\omega^2\varphi^3 + \ldots \quad (2)$$

If the φ^3 and higher order terms are neglected then the second-order approximation to Eq. (2) is amenable to an analytic asymptotic treatment described by Struble.[5]

It is assumed that the solution can be expressed as a series expansion in terms of the small parameter e,

$$\varphi = A_0\cos(\omega\nu - \theta) + A_1e + A_2e^2 + A_3e^3 + \ldots \quad (3)$$

where $A_o, \theta, A_1, A_2, A_3$ are treated as variables. The technique combines the use of variation of parameters as well as a perturbation method with the expansion in terms of e.

The process begins by substituting Eq. (3) into the approximation to Eq. (2) and equating like powers of eccentricity. This yields

$$[\ddot{A}_0 - A_0(\omega - \dot{\theta})^2 + \omega^2A_0]\cos(\omega\nu - \theta) = 0 \quad (4a)$$

$$[A_0\ddot{\theta} - 2\dot{A}_0(\omega - \dot{\theta})]\sin(\omega\nu - \theta) = 0 \quad (4b)$$

$$\ddot{A}_1 + \omega^2A_1 = 2[\dot{A}_0\cos(\omega\nu - \theta) + 1 - A_0(\omega - \dot{\theta})\sin(\omega\nu - \theta)]\sin\nu - [\ddot{A}_0 - A_0(\omega - \dot{\theta})^2]\cos(\omega\nu - \theta)\cos\nu - [A_0\ddot{\theta} - 2\dot{A}_0(\omega - \dot{\theta})]\sin(\omega\nu - \theta)\cos\nu \quad (4c)$$

$$\ddot{A}_2 + \omega^2A_2 = 2\sin\nu\dot{A}_1 - \ddot{A}_1\cos\nu \quad (4d)$$

Since A_o and θ determine the solution for zero eccentricity, they are treated as constants in Eq. (4c). This allows us to solve for A_1 which yields the solution to first order in eccentricity. Now we substitute the results in Eq. (3) and back in Eq. (2) and obtain a new set of variational equations similar to Eqs. (4a) and (4b) which are now complete to second order. The solution to these equations tells us that A_0 can be considered constant to second order (in eccentricity) but that θ varies as $e^2\nu$. The solution to Eq. (4d) can then be

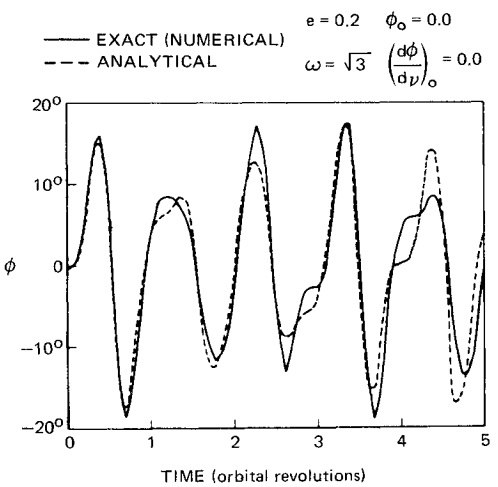

Fig. 1 Comparison of analytical and numerical solutions of Eq. (1).

Received February 10, 1971; revision received May 3, 1971. This work was done under U.S. Navy Contract N00017-62-C-0604 and supported by the Naval Air Systems Command. The authors thank Martins Sturmanis for doing the programing involved in this study.

* Senior Staff, Space Research and Analysis Branch; also Associate Professor of Mechanical Engineering, University of Maryland.
† Associate Physicist, Space Research and Analysis Branch.
‡ Mathematician, Space Research and Analysis Branch.